FRET-based method for direct, real-time measurement of DNA methyltransferase activity

Long, Yi; Ubych, Krystian; Jagu, Elodie; Neely, Robert K

DOI:
10.1021/acs.bioconjchem.0c00612

Document Version
Peer reviewed version

Citation for published version (Harvard):
Long, Y, Ubych, K, Jagu, E & Neely, RK 2021, 'FRET-based method for direct, real-time measurement of DNA methyltransferase activity', *Bioconjugate Chemistry*, vol. 32, no. 1, pp. 192-198. https://doi.org/10.1021/acs.bioconjchem.0c00612

A FRET-based method for direct, real-time measurement of DNA methyltransferase activity

Yi Long[1,2], Krystian Ubych[1], Elodie Jagu[1,3] and Robert K. Neely[1]

1. The University of Birmingham, School of Chemistry, Edgbaston, Birmingham, B15 2TT
2. Medical Research Center, Southern University of Science and Technology Hospital, Shenzhen, Guangdong Province, China, 518055
3. ICCF, SIGMA Clermont, Université Clermont Auvergne, CNRS, Clermont-Ferrand, 63178 Aubierre, France

ABSTRACT: DNA methyltransferase activity is associated with a host of diseases, including cancers, where global hypomethylation of the genome, as well as marked changes in local DNA methylation patterns can be both diagnostic and prognostic for the disease. Despite this we currently lack a method for directly measuring the activity of the DNA methyltransferases, which would support the development of DNA methyltransferase-targeted therapies. Here, we demonstrate an assay for the direct measurement of methyltransferase activity, in real-time. We employ a fluorescent methyltransferase cofactor analogue, which when bound by the enzyme to a labelled target DNA sequence results in fluorescence resonance energy transfer (FRET) between the donor dye (DNA) and the acceptor dye (cofactor). We demonstrate that the method can be used to monitor the activity of DNA MTases in real time and can be applied to screen inhibitors of the DNA methyltransferases. We show this in both bulk phase and single molecule imaging experiments, highlighting the potential application of the assay in screening and biophysical studies of methyltransferase function.

Introduction

Epigenetics refers to the study of heritable changes in phenotype, due to changes in the genome, that occur without altering the sequence of the DNA itself. [1] One of the most common and widely-studied epigenetic process is DNA methylation. In order for methylation to occur, a methyl group is transferred from the methyl-donor, *S*-adenosyl-L-methionine (AdoMet), to DNA by an enzyme, known as a DNA methyltransferase (DNA MTase). Both cytosine and adenine bases can be methylated, though cytosine methylation is far more common in eukaryotes than adenine methylation. [2, 3] In eukaryotes, DNA methylation plays a vital role in many biological processes including gene expression, maintenance of imprinted genes and X-chromosome inactivation. [4-6] Indeed, in humans, aberrant DNA methylation patterns, which are maintained by DNA methyltransferases, are associated with many different types of cancer. [7-9] For example, in human cells, the expression level of DNA(cytosine-5-)-methyltransferase 1 (DNMT1) was found to be up-regulated by a factor of 5.3 fold in leukemia. [10] DNA(cytosine-5-)-methyltransferase 3A (DNMT3A) and DNA(cytosine-5-)-methyltransferase 3B (DNMT3B) were found to be overexpressed in colon cancer. [11] Correspondingly, two small-molecule inhibitors of DNMTs, 5-Azacytidine (5azaC) and 5-Aza-2'-deoxycytidine (5azadC), have been approved by the FDA to treat leukaemia by inhibiting DNMT1. Several DNMT inhibitors are currently undergoing clinical trials. [12]

Despite the opportunity for developing novel therapies in this area, few assays that directly measure the activity of methyltransferases exist, and none to date show the potential to be applied at the single-molecule level and across complex sample types, such as cell lysates. This currently limits our ability to monitor directly the interaction between DNMTs and their substrates.

The gold-standard measure of methyltransferase activity uses radio-labeled AdoMet and gel electrophoresis to separate DNA and analyses labelling efficiencies. [13, 14] Alternative, indirect approaches focus on the analysis of the (by-)products of the methylation reaction, S-Adenosyl-L-homocysteine (AdoHcy), or methylated DNA. [15] Typically, these methods require several enzymatic steps and cannot be performed in complex mixtures, such as cell lysates, because of the presence of other enzymes producing, consuming and binding to AdoHcy. [15]

Detection of the product of the methylation reaction methylated DNA is possible using a host of technologies, including methylation-specific polymerase chain reaction (PCR), [16] high-performance liquid chromatography (HPLC), [17] and high performance capillary electrophoresis (HPCE). [18] However, these approaches are rather complex and poorly-suited to the type of high-throughput analysis that is necessary for companion diagnostics. [19] The high affinity of the methyl-binding domain (MBD) proteins toward methylated CpG sequences has been used to circumvent some of the limitations of these methods. [20] Despite this, MBD-based assays require more than one step and involve many other reagents in the reaction, making it difficult to apply them in a real-time kinetic assay for measuring the activity of the DNA MTases. To address this, several reports have presented methods for detecting methylation that rely on the ability of a restriction enzyme to recognise and cleave methylated DNA. For example, Jun et al. developed a fluorescent DNA hairpin probe-based method that measures DNA MTase activity in real-time. [21] Similarly, Robert et al. used hemi-methylated oligonucleotides to continuously monitor the activity of the bacterial cytosine-C5 methyltransferase M.SssI activity. [22] A sensitive, label-free and real time monitoring method for DNA MTase activity was developed based on the nanopore sensing technology. [23] Recently, Li-Juan, W. et al constructed a gold nanoparticle-based nanosensor that can detect multiple DNA MTase enzymes at the single molecule level, simultaneously. Zi-yue, W. et al have recently reported a chemiluminescent sensor for bacteria and human DNA MTase quantification. [24, 25] Although great progress has been made in the development of real-time DNA MTase activity methods, the requirement for restriction endonucleases in these assays limits their application in compound screening, as the restriction endonuclease may be sensitive to antitumor drugs. [14, 19]

Previous studies have displayed direct and real-time observation methyltransferase activity through application of the fluorescent nucleic acid base analogue, 2-Aminopurine (2AP). [26, 27] However, this approach lacks specificity (DNA polymerases, endonucleases, and the uracil DNA glycosylases all perturb DNA in a similar fashion). [28] In addition, the low fluorescence quantum yield of 2AP and its requirement for UV excitation prevent application of the probe in single-molecule and microscopic studies. [29]

Hence, there remains a pressing need to develop methods for directly measuring the activity of DNA MTases in real-time and with high specificity for high-throughput assays. Recently, we described the application of AdoMet analogues for the alkylation (as opposed to methylation) of DNA with complex moieties from polymers to fluorophores. [30] Inspired by this, we have developed a one pot, direct method for monitoring MTase activity using fluorescence resonance energy transfer (FRET). We show that measurement of the FRET efficiency of the system allows estimation of the kinetic activity of the prototypical M.TaqI methyltransferase enzyme. We extend this to investigate inhibition of enzymatic activity by two AdoMet analogues, highlighting the method's suitability for use in screening for DNA methyltransferase inhibitors. Finally, we show that the enzymatic product can be detected using single-molecule imaging, allowing further insight into the behaviour of these enzymes.

Results and Discussion

We aimed to develop a one step and real time method for methyltransferase activity measurement, as depicted in Figure 1.

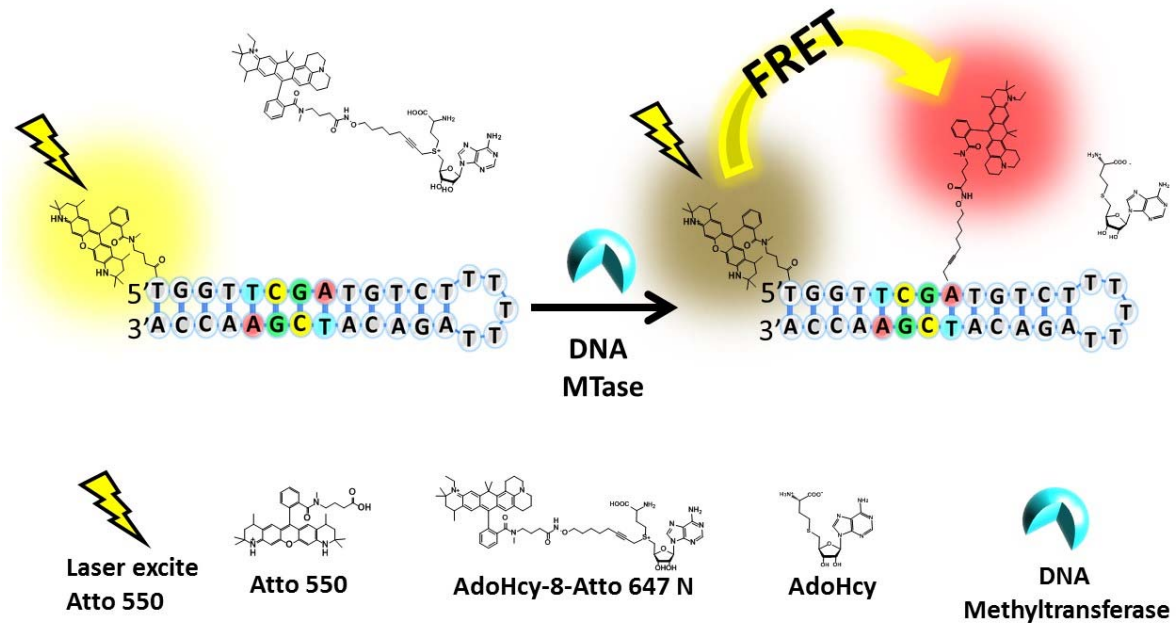

Figure 1. Illustration of the approach for FRET-based real time measurement of methyltransferase activity. DNA is labeled with a donor fluorophore (Atto550) and carries a recognition site for a methyltransferase enzyme and the cofactor analogue carries an acceptor fluorophore (Atto647N). FRET occurs only once the ternary DNA-MTase-cofactor complex is formed.

A donor fluorophore (Atto550) was attached to a DNA hairpin probe containing a recognition site for the M.TaqI DNA methyltransferase enzyme. The acceptor fluorophore (Atto647N) was added to the cofactor analogue, which is carried to the DNA hairpin by the methyltransferase and is subsequently covalently bound to the adenine base of the enzyme's recognition site (5'-TCGA-3'). The enzyme can bind in either orientation to this site, and the close proximity of the site to the Atto550 dye (< 3 nm) means that the fluorophores are well within their reported Förster radius of 6.5 nm (Atto-tec). We also found that this pair provided a FRET signal that was robust towards the elevated temperatures used for the M.TaqI reaction (50°C).

Upon enzyme binding to its target site on the hairpin, donor and acceptor lie < 3 nm apart and efficient FRET is observed, Figure 2. In the absence of the methyltransferase enzyme, the AdoHcy-8-Atto647N cofactor analogue diffuses freely and the distance between Atto550 and Atto647N dyes is too great for FRET to be observed, Figure 2.

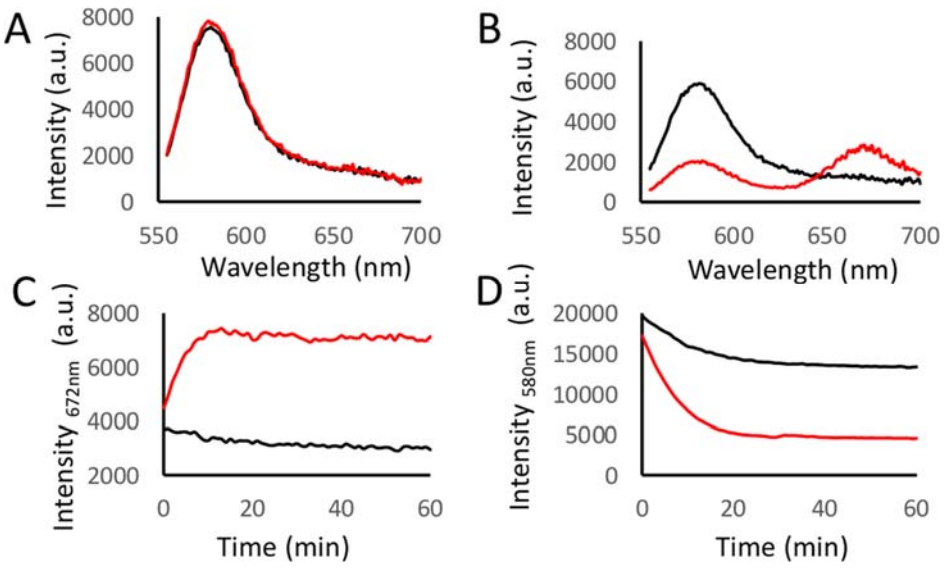

Figure 2. Top panels: Fluorescence emission spectra of the samples with (red line) or without (black line) M.TaqI in the reaction mixture. Spectra are recorded at the start (A) and end (B) of the transalkylation reaction. Bottom panels: Kinetic measurements with (red line) or without (black line) M.TaqI in the reaction mixture. Fluorescence intensity was recorded over time for Atto647N (C) or Atto 550 (D) emission.

Monitored in real-time, the fluorescence intensity, centred at 672 nm, increases rapidly, suggesting that under these conditions the reaction is complete after approximately 10 minutes. A corresponding decrease in the intensity of the donor fluorophore is observed. We also note that the fluorescence intensity of the donor fluorophore decreases over time, most likely due to thermal degradation of the fluorophore and photobleaching during the measurement. We compensate for this in subsequent calculations by using ratios of the acceptor:donor emission intensities. The reaction can also be monitored by UV-Vis absorption, Figure S6. Initial experiments using a second DNA MTase, M.MpeI, were undertaken, Figure S7. M.MpeI apparently shows a weaker binding affinity for this cofactor than M.TaqI, and, as a result, a much lower FRET signal. The approach is likely to require further optimisation for other methyltransferases, however, this also suggests that some specificity for a target methyltransferase may be achieved.

In order to verify transalkylation of DNA by M.TaqI in the presence of the AdoHcy-8-Atto647N cofactor analogue, we purified the product of the reaction and immobilised this on a glass cover slide for single-molecule imaging, Figure 3.

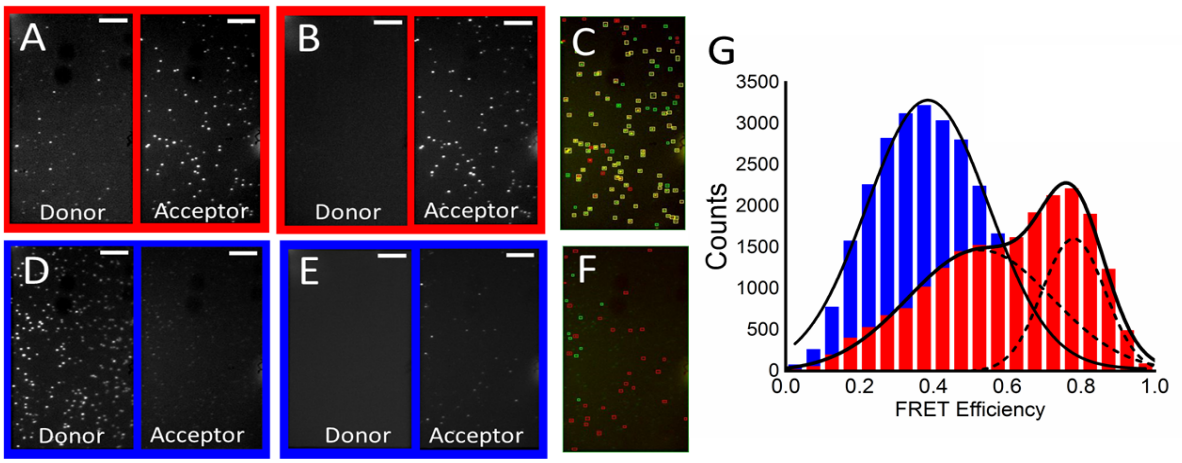

Figure 3. Fluorescence image of reaction product where panels A-D show emission from the donor (left) and acceptor (right) channels. A control sample, without addition of methyltransferase is also shown (blue). The scale bar is 8 µm. Panels A-C: Labelled hairpin probe. (A) Excitation of labelled hairpin probe at 561 nm, (B) excitation of labelled hairpin probe at 640 nm. (C) an overlay of the acceptor channels from (A) and (B). Panels D-F: Control sample with no M.TaqI in the reaction mixture. (D) Excitation of hairpin probe at 561 nm, (E) excitation of hairpin probe at 640 nm. (F) an overlay of the acceptor channels from (D) and (E). (G) FRET efficiencies derived from analysis of the over 200 FRET pairs for the reaction product (red) and control without addition of methyltransferase (red). Data was analysed using iSMS software. Histograms were fitted using Gaussian distribution using Origin 2018.

Figure 3 (A-C) are images taken for the labelled DNA probe and (D-F) are images from a control sample, where M.TaqI was omitted from the labelling reaction. In each of the panels A, B, D and E, donor emission channels are on the left half side with and acceptor emission channels are on the right half side. Figure 3A, shows efficient FRET occurring for the reaction product with excitation of the donor at 561 nm, since few donor molecules but many acceptors are emitting. Conversely, for the unlabelled, control sample (Figure 3D), no emission from the acceptor channel is observed with excitation of the donor fluorophore. Colocalisation analysis for the reaction product shows good overlap, of emitters excited by FRET (561 nm), and by direct excitation of the acceptor (640 nm), with 88 ± 2% of emitters being colocalised. Conversely, from the control sample, no colocalization was seen between the emitters with excitation in the 561 nm and 640 nm channels. Hence, we confirm that efficient transalkylation occurs, with a high labelling efficiency.

We further quantified the observed FRET efficiencies for emitters in these single-molecule movies, Figure 3G and Supplementary Figure S8, using open-source iSMS software.[31] Figure 3G shows the determined distributions of FRET efficiencies for the reaction product (red) and control sample (blue). The reaction product shows a clear shift towards higher FRET efficiencies than the control sample. Furthermore, two distinct populations of molecules are seen in the reaction product, one high FRET efficiency, centred on an efficiency of 0.78 ± 0.002 and one with an intermediate FRET efficiency centred on 0.53 ± 0.013. The M.TaqI target site begins just five bases from the terminus of the hairpin that carries the Atto555 donor fluorophore. The site (5'-TCGA-3', where the adenine is the target base for labelling) is palindromic and can carry either one two fluorophores, where either one or both of the adenine bases are labelled. We expect labels on either of the two targetable adenine bases to result in the high FRET state, since the Förster radius for the Atto555-Atto647N pair is 6.5 nm (Atto-tec). The population of hairpins with an intermediate FRET efficiency could be due to hairpin melting, conformational confinement of one or more of the dyes or the presence of two acceptor dyes on both target adenine bases and corresponding multiple energy-transfer events (donor-acceptor-acceptor) taking place.

Following the single-molecule studies, we undertook more in-depth kinetic studies using this approach. Figure 4 shows the kinetic traces for the transalkylation reaction at a range of different enzyme concentrations. Whilst the raw data (Figure 4A and 4B) shows a rather complex response of the fluorescence intensity to reaction progression, the ratiometric analysis of these traces (Figure 4C) shows linear dependence of the reaction rate on enzyme concentration (Figure S9). Plots (Figure 4C) for all enzyme concentrations are close to linear in the first 20 minutes of the reaction and plateau at different times thereafter, suggesting that the substrate is consumed gradually over time under all of the tested conditions. A linear plot result (Figure S9) for F672nm/F580 versus different concentration of M.TaqI at the reaction time of 20 minutes, 40 minutes and 60 minutes suggests that the

concentration dependence linear range changes with time, which will help us construct a standard curve for enzyme concentration determination.

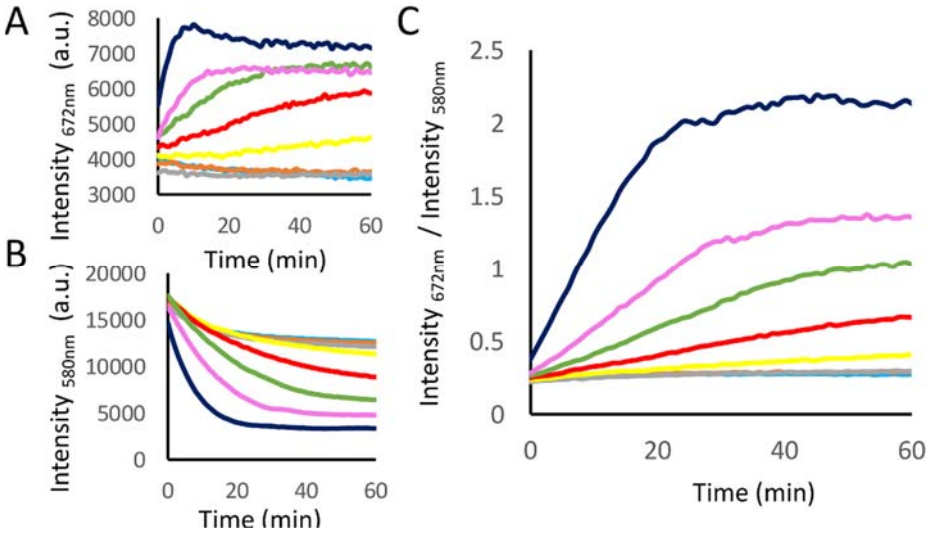

Figure 4. Kinetic measurement of M.TaqI catalytic rates for a range of enzyme concentrations. 0 nM (light blue), 12.5 nM (orange), 25 nM (grey), 50 nM (yellow), 100 nM (red), 200 nM (green), 400 nM (pink), 800 nM (dark blue). Change in fluorescence intensity over time for acceptor (A) and donor (B) fluorophores. (C) The calculated ratio of the fluorescence intensities of acceptor: donor fluorophores over time (data shown in the figure is the average intensity from 3 replicates).

The detection limit of our approach was also obtained using the data from this experiment. A threshold value for the detection limit was set for a given time point as the signal from control plus three standard deviations. For example, for the time point at 20 minutes, this threshold was calculated as 0.32 for the F672nm/F580nm ratio. Under these conditions, the experiments containing 50 nM and 100 nM of M.TaqI gave F672nm/F580nm ratios of 0.31 and 0.40 respectively. Hence, we estimate a limit of detection for the assay of 100 nM enzyme, where the reaction is allowed to proceed for 20 minutes. With longer reaction times, e.g. at 40 minutes, the limit of detection drops to 50 nM M.TaqI. It can be seen that, since the product formation is irreversible, sensitivity can be improved simply by prolong the reaction time.

We determined the dependence of the transalkylation reaction rates on the substrate (AdoHcy-8-Atto647N and DNA) concentrations, Figure 5. Using this data, we can determine pseudo-Michaelis-Menten parameters for the reaction, where the reaction 'product' is the formation of the ternary [M.TaqI]-[AdoHcy-8-Atto647N]-[DNA] complex, that gives rise to the FRET signal we record. Hence, for the [AdoHcy-8-Atto647N] cofactor, we obtain a K_M =10.4 ± 4.0 µM (mean ± standard error) and V_{max} = 1.2 ± 0.3 µM/min, Figure 5A. Similarly, for the DNA hairpin probe we derive K_M = 360 ± 110 nM and V_{max} = 92 ± 9 nM/min, Figure 5B.

As might be anticipated, the derived K_M for our bulky cofactor analogue is approximately three-fold lower than that reported for AdoMet binding to M.TaqI (K_M = 3.7 ± 1.1 µM). [32] However, K_M for the DNA molecule is similar to previously reported values (600 ± 200 nM), indicating that the bulky cofactor analogue has little impact on the ability of M.TaqI to bind its target DNA.

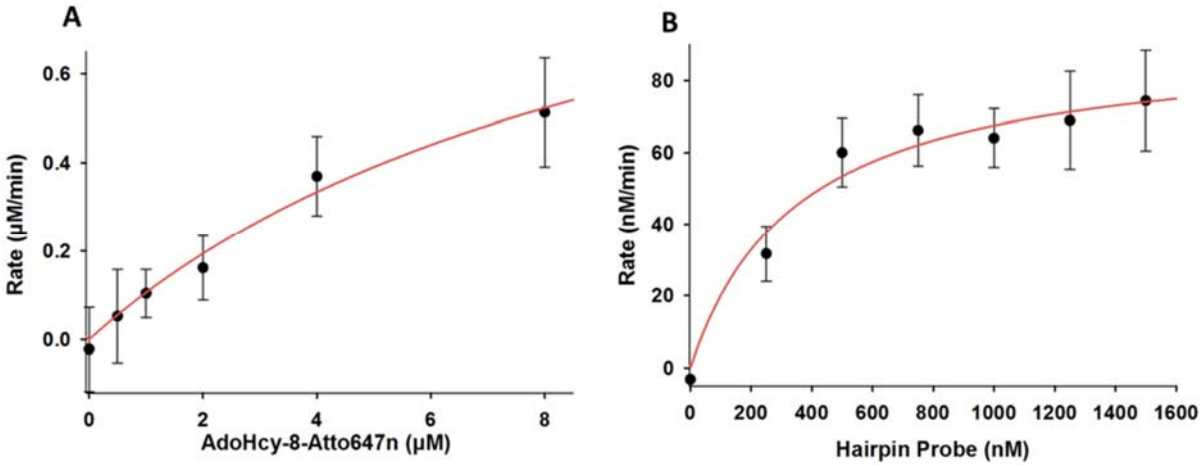

Figure 5. Analysis of Michaelis-Menten kinetic parameters for substrates by present method. (A) Effect of AdoHcy-8-Atto647N concentration on velocity of reaction. 0, 0.5, 1, 2, 4, 8 µM of AdoHcy-8-Atto647N were reacted with 1 µM hairpin probe and 800 nM M.TaqI. Reaction velocity was plotted against the concentration of AdoHcy-8-Atto647N and fitted by Michaelis-Menten equation. (B) Different concentration of hairpin probe with 0, 250, 500, 750, 1000, 1250 and 1500 nM were added in reactions contained 8 µM AdoHcy-8-Atto647N and 800 nM M.TaqI. The average velocity was plotted against different concentration of AdoHcy-8-Atto647N and fitted by Michaelis-Menten equation. Results are derived from three replicates of experiment and are shown with the standard error bar.

Raw data underpinning these reactions is shown in Figure S10. We note that at the highest enzyme concentration tested (16µM), the emission intensity of the acceptor dye shows anomalous behaviour increasing to a maximum value and subsequently falling as the reaction progresses. We attribute this to the addition of a second fluorophore to the hairpin probe by the M.TaqI and speculate that interaction between these closely-spaced (4 base pairs, 1.5 - 2 nm) Atto647N fluorophores leads to some quenching of their fluorescence emission. This trace was omitted from the calculation of the Michaelis-Menten parameters and negating this effect will be an important consideration for future work.

Ultimately, we aim to employ this assay to improve screening for DNA methyltransferase inhibitors. To demonstrate the potential for our method in drug screening, sinefungin and AdoHcy were used to as model inhibitors to establish the impact of competitive (drug) binding at the cofactor pocket of our methyltransferase.

We monitored the ratio of acceptor:donor emission intensity with varying concentration of inhibitors to determine IC_{50} values for both sinefungin and AdoHcy for M.TaqI. Figure 6 shows dose-dependent curves for titration of both inhibitors into a series of transalkylation reactions. We express the inhibition efficacy as a "percent activity" (%A) for the reaction, which is calculated as a fraction of the FRET signal from the sample, relative to two control samples: %A = ((signal sample) – (signal completely inhibited sample))/((no inhibitor sample) – (completely inhibited sample)) x 100. Raw data for these experiments can be found in Figure S11, where the signal of F647nm/F580nm is plotted against time and is the average over three independent experiments. The percentage activity of M.TaqI was calculated using acceptor:donor intensity ratios after 20 minutes of reaction. From this, we determined an IC_{50} for sinefungin of 61 ± 28 (mean ± Standard Error) µM and for AdoHcy, an IC_{50} value of 190 ± 80 µM. As anticipated, the IC_{50} value calculated for sinefungin is somewhat lower than that we derive for AdoHcy. This implies that sinefungin is a stronger inhibitor for M.TaqI activity, compared to AdoHcy. This result in good agreement with the literature. [33] This pilot test demonstrates

the suitability of this method for measuring inhibitor potency profile and has great potential for high throughput drug screening in the future.

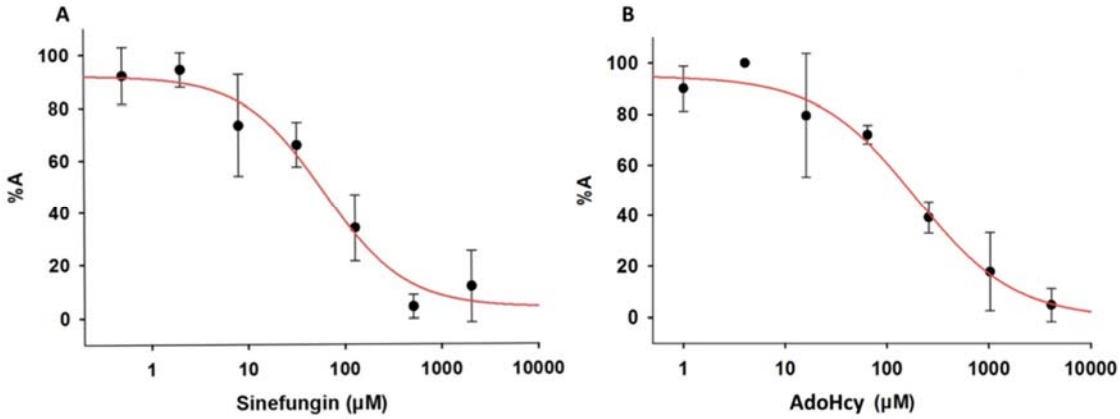

Figure 6. Assay of the inhibition of M.TaqI by the present method. Inhibitors were reacted with 1 µM hairpin probe, 8 µM AdoHcy-8-Atto647N, and 200 nM M.TaqI (A) Dose-dependent curve for sinefungin at concentrations of 0.5, 2, 8, 32, 128, 512, 2048 µM. (B) Inhibition profile of AdoHcy at concentrations of 1, 4, 16, 64, 256, 1024, 4096 µM. The result is shown is for three replicates of experiment and displayed with the standard error bar.

Conclusions

Methyltransferase enzymes play important roles in epigenetic changes which can affect gene transcription and parental imprinting and have been implicated as drivers of a range of diseases, including cancer. Furthermore, there are hundreds of clinical trials in progress that employ demethylating agents for 'epigenetic priming', with the aim of improving the performance of more targeted therapies. Thus, methyltransferases are an emerging class of enzymes that are important targets for drug discovery. Using M.TaqI as a model enzyme, here we have developed a simple and straightforward assay that can measure activity of methyltransferase in one pot with one step in real time. We demonstrated the validity of our approach both in the bulk phase using a fluorescence measurement on microplate reader and on the fluorescence microscope, at the single-molecule level.

Our method has many advantages compared to currently available assays for methyltransferase activity: The FRET signal is extremely specific to cofactor molecules bound to their DNA targets and hence, is compatible with assays performed in complex mixtures, such as cell lysates; the reaction system is very simple, containing only two substrates in solution and odes not rely on the activity of other enzymes, such as restriction enzymes; the approach is quick and easy to handle with low sample volumes and nanomolar concentrations of methyltransferase. Finally, we have shown that our approach can be applied at the single-molecule level and, in the future, can be applied to study the heterogeneity of dynamic behaviours within populations of methyltransferase complexes. Hence, we believe this method can be used for study of the kinetic activity of methyltransferases in real time and in a high throughput format adapted for drug screening.

Experimental Section

Reagents and Materials: M.TaqI was extracted and purified according the previously described procedure.[34] The hairpin DNA probe 5'-(Atto550)- TGGGTTCGATGTCTTTTTAGACATCGAACCCA-3'was

synthesized by Integrated DNA Technologies (IDT). Reagents were purchased from Sigma-Aldrich and used according to the manufacturer's instructions, unless stated otherwise. CutSmart® buffer, pUC19 plasmid, proteinase K, R.HaeII and R.TaqαI (R.TaqI) were purchased from New England BioLabs (NEB). Atto647N-NHS ester was from ATTO-TEC GmbH. Ultravision plate 384 (4ti-0214) is a product from 4titude® Limited. CLARIOstar microplate reader is a product from BMG LABTECH Ltd. MS spectra were obtained on a Xevo® G2-XS-ToF (Waters) and Synapt-G2-S from electrospray ionization (ESI) and time-of-flight (TOF) measurement in negative or positive ion mode. Analytical RP-HPLC was performed on Schimadzu LC-20 Prominence equipped with ACE 5 C18 (250 x 4.6 mm, flow rate 1 ml/min). Elution with 10 mM ammonium acetate pH 5.5/MeCN gradient: 3-100% MeCN over 60 minutes. Preparative RP HPLC was performed on Agilent Technologies 1260 Infinity equipped with ACE 5 C18 (250 x 21.2 mm, 100 Å, flow rate 10 ml/min). Elution with 10 mM ammonium acetate pH 5.5/MeCN gradient: 3-100% MeCN over 60 minutes. The UV-detection was carried at 260 nm and 647 nm. The concentration and yield were determined by UV absorbance measurements at 647 nm performed in 0.1 % acetic acid. For the calculation, molar extinction coefficient was used: A_{647} = 150000 mol^{-1} cm^{-1}.

Synthesis of AdoHcy-8-Atto647N: Synthesis of the hydroxylamine derivative cofactor AdoHcy-8-ONH2 was as described previously.[34] This highly reactive cofactor was immediately coupled to the commercial Atto647N-NHS ester (50mM, DMSO solution) in PBS buffer (6mM final concentration), Figure S1. The mixture was stirred for 30 min at room temperature in dark. The resulting AdoHcy-8-Atto647N cofactor was directly injected into the HPLC for purification. HPLC gradient: MeOH Ammonium Formate 3-100% in 60min. AdoHcy-8-Atto647n cofactor was collected, freeze dried and characterised by mass analysis. The resulting blue solid was dissolved in 100µL 0.1% formic acid and concentration was determinate by measuring absorbance. Yield 12%. MS: m/2 [M+H] = 576.32. HRMS: Found 1152.6202 for 1152.6164 calculated mass, molecular formula C64H84N10O8S. HPLC and mass spectrum results can be found in Figures S2 and S3.

The ability of M.TaqI to catalyse transalkylation of DNA using AdoHcy-8-Atto647N as a cofactor analogue was tested using the corresponding restriction enzyme (R.TaqαI) to challenge the alkylated DNA. Gel electrophoresis used to analyse the digestion pattern of the DNA. A full description of the method and result can be found in Figure S4.

Activity Assay of of M.TaqI: The real time activity assay of M.TaqI was carried out using an Ultravision plate 384 at 50°C in 30 µL volume. Each reaction contains 1x CutSmart buffer, and varying concentrations of hairpin probe, AdoHcy-8-Atto647N and M.TaqI. After each reagent was mixed in the wells and sealed using qPCR seal, the plate was placed in CLARIOstar microplate reader to record fluorescence spectra and time-courses. Bottom optic settings were used with a focal height set to 5mm. For the kinetic measurements using Atto550 labelled hairpin probe, the excitation wavelength was set to 512nm with slit width of 25nm, while the emission was measured at 580nm with a slit width of 30nm. The dichroic filter was set at 541.2nm and gain was set at 1500. Kinetic measurements of the AdoHcy-8-Atto647N also used an excitation wavelength of 512nm with a slit width of 25nm, while the emission was measured at 672nm with slit of 35nm. The dichroic filter was set at 600nm and gain was set at 2000. Steady-state fluorescence spectra were recorded using an excitation wavelength of 512 nm and slit width of 25nm. Fluorescence emission intensity was recorded from 555nm to 700nm with a 25nm slit width. Gain was set at 1500 and focal height was 5mm.

Detection of reaction product using fluorescence imaging: 30 ul mixtures consisting of 1x CutSmart buffer, 1µM hairpin probe, 8µM AdoHcy-8-Atto647N and 800nM M.TaqI were reacted at 50°C for 1 hour. After the reaction, two tubes of reaction product were combined and purified using a QIAquick kit (Qiagen). DNA was eluted from the column in 50 ul H_2O. The purified labelled DNA was diluted 10^{-}

^{5} fold in 1x CutSmart buffer to approximately 10pM. Cleaned glass slides were coated with 0.01% poly-l-lysine. Finally, 5µl of the DNA solution was applied to the treated glass slides.

Slides were imaged on an ASI RAMM microscope, equipped with a Nikon 100× 1.45 NA TIRF objective. Illumination was from a 50 mW OBIS 561 nm or a 100 mW OBIS 640 nm CW laser (Coherent) via a quad-band dichroic mirror (405/488/561/635). Power at the sample was approximately 1mW. The fluorescence signals from the fluorophores were separated by Optosplit II image splitter (Cairn Research) using a 624 nm edge BrightLine single-edge dichroic beamsplitter (Semrock), and imaged onto the two halves of an Evolve Delta EM-CCD camera using a 50 ms exposure and camera gain of 50. Data analysis was performed using spots colocalization (ComDet v.0.4.1) plugin in Image J. A maximum distance between colocalized spots of 4 pixels for the colocalization calculation. An open-source version of iSMS package in Matlab was used for generate single-molecule FRET imaging traces. Origin 2018 was used for Gaussian distribution analysis.

Conflicts of interest

The authors declare no competing interests.

Acknowledgment

This work was supported by the Engineering and Physical Sciences Research Council (EPSRC, grant number EP/N020901/1).

Supporting Information

The Supporting Information is available free of charge at xxxxxxxxxxx

- Reagents and Materials
- Experimental details and supporting results

Notes and references

1. Gnyszka, A., Z. JASTRZĘBSKI, and S. Flis, *DNA methyltransferase inhibitors and their emerging role in epigenetic therapy of cancer.* Anticancer research, 2013. **33**(8): p. 2989-2996.
2. Willbanks, A., M. Leary, M. Greenshields, C. Tyminski, S. Heerboth, K. Lapinska, K. Haskins, and S. Sarkar, *The evolution of epigenetics: from prokaryotes to humans and its biological consequences.* Genetics & epigenetics, 2016. **8**: p. GEG. S31863.
3. Sánchez-Romero, M.A., I. Cota, and J. Casadesús, *DNA methylation in bacteria: from the methyl group to the methylome.* Current opinion in microbiology, 2015. **25**: p. 9-16.
4. Razin, A. and H. Cedar, *DNA methylation and gene expression.* Microbiological reviews, 1991. **55**(3): p. 451-458.
5. Li, E., C. Beard, and R. Jaenisch, *Role for DNA methylation in genomic imprinting.* Nature, 1993. **366**(6453): p. 362.
6. Hellman, A. and A. Chess, *Gene body-specific methylation on the active X chromosome.* science, 2007. **315**(5815): p. 1141-1143.
7. Chatterjee, A., E.J. Rodger, and M.R. Eccles. *Epigenetic drivers of tumourigenesis and cancer metastasis*. in *Seminars in cancer biology*. 2018. Elsevier.
8. Ehrlich, M., *DNA methylation in cancer: too much, but also too little.* Oncogene, 2002. **21**(35): p. 5400.

9. Subramaniam, D., R. Thombre, A. Dhar, and S. Anant, *DNA methyltransferases: a novel target for prevention and therapy.* Frontiers in oncology, 2014. **4**: p. 80.
10. Mizuno, S.-i., T. Chijiwa, T. Okamura, K. Akashi, Y. Fukumaki, Y. Niho, and H. Sasaki, *Expression of DNA methyltransferases DNMT1, 3A, and 3B in normal hematopoiesis and in acute and chronic myelogenous leukemia.* Blood, 2001. **97**(5): p. 1172-1179.
11. Robertson, K.D., E. Uzvolgyi, G. Liang, C. Talmadge, J. Sumegi, F.A. Gonzales, and P.A. Jones, *The human DNA methyltransferases (DNMTs) 1, 3a and 3b: coordinate mRNA expression in normal tissues and overexpression in tumors.* Nucleic acids research, 1999. **27**(11): p. 2291-2298.
12. Pechalrieu, D., C. Etievant, and P.B. Arimondo, *DNA methyltransferase inhibitors in cancer: from pharmacology to translational studies.* Biochemical pharmacology, 2017. **129**: p. 1-13.
13. Jurkowska, R.Z., A. Ceccaldi, Y. Zhang, P.B. Arimondo, and A. Jeltsch, *DNA methyltransferase assays*, in *Epigenetics Protocols*. 2011, Springer. p. 157-177.
14. Gros, C., L. Chauvigne, A. Poulet, Y. Menon, F. Ausseil, I. Dufau, and P.B. Arimondo, *Development of a universal radioactive DNA methyltransferase inhibition test for high-throughput screening and mechanistic studies.* Nucleic acids research, 2013. **41**(19): p. e185-e185.
15. Gros, C., J. Fahy, L. Halby, I. Dufau, A. Erdmann, J.-M. Gregoire, F. Ausseil, S. Vispé, and P.B. Arimondo, *DNA methylation inhibitors in cancer: recent and future approaches.* Biochimie, 2012. **94**(11): p. 2280-2296.
16. Herman, J.G., J.R. Graff, S. Myöhänen, B.D. Nelkin, and S.B. Baylin, *Methylation-specific PCR: a novel PCR assay for methylation status of CpG islands.* Proceedings of the national academy of sciences, 1996. **93**(18): p. 9821-9826.
17. Eick, D., H.-J. Fritz, and W. Doerfler, *Quantitative determination of 5-methylcytosine in DNA by reverse-phase high-performance liquid chromatography.* Analytical biochemistry, 1983. **135**(1): p. 165-171.
18. Fraga, M.F., R. Rodríguez, and M.J. Cañal, *Rapid quantification of DNA methylation by high performance capillary electrophoresis.* ELECTROPHORESIS: An International Journal, 2000. **21**(14): p. 2990-2994.
19. Poh, W.J., C.P.P. Wee, and Z. Gao, *DNA methyltransferase activity assays: advances and challenges.* Theranostics, 2016. **6**(3): p. 369.
20. Xu, Z., H. Yin, L. Huo, Y. Zhou, and S. Ai, *Electrochemical immunosensor for DNA methyltransferase activity assay based on methyl CpG-binding protein and dual gold nanoparticle conjugate-based signal amplification.* Sensors and Actuators B: Chemical, 2014. **192**: p. 143-149.
21. Li, J., H. Yan, K. Wang, W. Tan, and X. Zhou, *Hairpin fluorescence DNA probe for real-time monitoring of DNA methylation.* Analytical chemistry, 2007. **79**(3): p. 1050-1056.
22. Wood, R.J., J.C. McKelvie, M.D. Maynard-Smith, and P.L. Roach, *A real-time assay for CpG-specific cytosine-C5 methyltransferase activity.* Nucleic acids research, 2010. **38**(9): p. e107-e107.
23. Rauf, S., L. Zhang, A. Ali, J. Ahmad, Y. Liu, and J. Li, *Nanopore-based, label-free, and real-time monitoring assay for DNA methyltransferase activity and inhibition.* Analytical chemistry, 2017. **89**(24): p. 13252-13260.
24. Wang, L.-J., X. Han, J.-G. Qiu, B. Jiang, and C.-Y. Zhang, *Cytosine-5 methylation-directed construction of a Au nanoparticle-based nanosensor for simultaneous detection of multiple DNA methyltransferases at the single-molecule level.* Chemical Science, 2020. **11**(35): p. 9675-9684.
25. Wang, Z.-y., P. Li, L. Cui, Q. Xu, and C.-y. Zhang, *Construction of a universal and label-free chemiluminescent sensor for accurate quantification of both bacteria and human methyltransferases.* Analytical Chemistry, 2020. **92**(19): p. 13573-13580.

26. Gerasimaitė, R., E. Merkienė, and S. Klimašauskas, *Direct observation of cytosine flipping and covalent catalysis in a DNA methyltransferase.* Nucleic acids research, 2011. **39**(9): p. 3771-3780.
27. Holz, B., E. Weinhold, S. Klimasauskas, and S. Serva, *2-Aminopurine as a fluorescent probe for DNA base flipping by methyltransferases.* Nucleic acids research, 1998. **26**(4): p. 1076-1083.
28. Wilhelmsson, M., *Fluorescent nucleic acid base analogues.* Quarterly reviews of biophysics, 2010. **43**(2): p. 159-183.
29. Neely, R. and A. Jones, *2-aminopurine as a fluorescent probe of DNA conformation and the DNA–enzyme interface.* interface, 2015. **48**(2): p. 244-279.
30. Lauer, M.H., C. Vranken, J. Deen, W. Frederickx, W. Vanderlinden, N. Wand, V. Leen, M.H. Gehlen, J. Hofkens, and R.K. Neely, *Methyltransferase-directed covalent coupling of fluorophores to DNA.* Chemical science, 2017. **8**(5): p. 3804-3811.
31. Preus, S., Noer, S.L., Hildebrandt, L.L., Gudnason, D., Birkedal, V.,, *iSMS: single-molecule FRET microscopy software.* Nature Methods, 2015(12).
32. Pues, H., N. Bleimling, B. Holz, J. Wölcke, and E. Weinhold, *Functional roles of the conserved aromatic amino acid residues at position 108 (motif IV) and position 196 (motif VIII) in base flipping and catalysis by the N6-adenine DNA methyltransferase from Thermus aquaticus.* Biochemistry, 1999. **38**(5): p. 1426-1434.
33. Schluckebier, G., M. Kozak, N. Bleimling, E. Weinhold, and W. Saenger, *Differential binding of S-adenosylmethionine S-adenosylhomocysteine and Sinefungin to the adenine-specific DNA methyltransferase M. TaqI.* Journal of molecular biology, 1997. **265**(1): p. 56-67.
34. Andrew A., W., J. Elodie, U. Krystian, R. Ashleigh E., K. Jack, S. Qiang, N. Robert K., and F.-T. Paco, *Site-Selective and Re-Writable Labelling of DNA Through Enzymatic, Dynamic and Click Chemistries*. 2019.